Physica A 387 (2008) 6845–6856

Contents lists available at ScienceDirect

Physica A

journal homepage: www.elsevier.com/locate/physa

A new macro model with consideration of the traffic interruption probability

T.Q. Tang [a,b], H.J. Huang [b,*], G. Xu [b]

[a] School of Transportation Science and Engineering, Beijing University of Aeronautics and Astronautics, Beijing 100083, China

[b] School of Economics and Management, Beijing University of Aeronautics and Astronautics, Beijing 100083, China

ARTICLE INFO

Article history:
Received 25 April 2008
Received in revised form 19 August 2008
Available online 6 September 2008

PACS:
89.40.-a
45.70.Vn
05.70.Fh

Keywords:
Traffic flow
Interruption probability
Car-following behavior
Macro model
Linear stability analysis
Simulation

ABSTRACT

In this paper, we present a new macro model which involves the effects that the probability of traffic interruption has on the car-following behavior through formulating the inner relationship between micro and macro variables. Linear stability analysis shows that consideration of the traffic interruption probability can improve the stability of traffic flow if and only if the drivers' reactive time required for adjusting their acceleration based on the traffic interruption probability p is not greater than that one based on the non-interruption probability $1 - p$. Numerical results verify that the new model can be used to analyze the effects of traffic interruption probability and traffic interruption on shock, rarefaction wave, small perturbation and uniform flow. The model has been applied in reproducing some complex traffic phenomena resulted by some traffic interruptions (*e.g.*, signal light, pedestrian and tolling station).

1. Introduction

Many traffic flow models have been developed to describe the physical mechanisms of various complex traffic phenomena [1–16] (*e.g.*, the formation mechanism and the propagating properties of various traffic waves and jams, the mechanisms of lane-changing and overtaking, the interactions among multiple vehicles). However, the existing models do not involve the effects of traffic interruption probability on traffic flow, and then can not directly be used to study the complex traffic phenomena resulted by various traffic interruptions. In fact, some traffic interruptions (*e.g.*, accidents) always occur with some probabilities and produce complex phenomena. Wong et al. [17–19] studied the contributing factors to traffic accidents. Telesca and Lovallo [20] analyzed the temporal properties in traffic accident time series and found that the time dynamics of traffic accidents is not Possonian but long-range correlated with periodicities ranging from 12 h to one year. Recently, Baykal-Gürsoy et al. [21] used the queuing theory to model traffic flow interrupted by incidents. The models proposed in Refs. [17–21] can reproduce some traffic phenomena resulted by accidents, but can not be used to evaluate the effects of various traffic interruption factors on the dynamic properties of traffic flow, since the traffic interruption probability is not considered explicitly.

In this paper, we first analyze the effects that the probability of traffic interruption has on the car-following behavior. Based on the inner relationship between micro and macro variables [22], we develop a new macro model with consideration of the traffic interruption probability. Then, we numerically investigate the effects that the traffic interruption probability

* Corresponding author.
E-mail address: haijunhuang@buaa.edu.cn (H.J. Huang).

0378-4371/$ – see front matter © 2008 Elsevier B.V. All rights reserved.
doi:10.1016/j.physa.2008.08.036

and one traffic interruption (*e.g.*, accident) have on the stability of traffic flow, shock, rarefaction wave, small perturbation and uniform flow. Finally, we apply our model to analyze the complex traffic phenomena caused by some traffic interruptions (*e.g.*, signal light, pedestrian and tolling station).

2. The car-following model

In general, the single-lane car-following model can be written as follows [1]:

$$\frac{\mathrm{d}^2 x_n}{\mathrm{d}t^2} = f\left(v_n, \Delta x_n, \Delta v_n\right), \tag{1}$$

where f is the stimulus function, x_n and v_n are the position and speed of the nth vehicle respectively, $\Delta x_n = x_{n+1} - x_n$ is the headway, $\Delta v_n = v_{n+1} - v_n$ is the relative speed. Eq. (1) states that the acceleration of a vehicle is determined by the speed v_n, the headway Δx_n and the relative speed Δv_n. In order to improve the stability of traffic flow, scholars later developed some improved car-following models as follows [23–27]:

$$\frac{\mathrm{d}^2 x_n}{\mathrm{d}t^2} = f\left(v_n, \Delta x_n, \Delta x_{n+1}, \ldots, \Delta x_{n+m}, \Delta v_n\right), \tag{2}$$

where $\Delta x_{n+i} = x_{n+i+1} - x_{n+i}$. Zhao and Gao [28] found that a collision will occur under certain given conditions when using the FVD (full velocity difference) model [29] to describe traffic flow. They then proposed a new model with consideration of the effects that the acceleration of the leading vehicle has on the following vehicle, *i.e.*,

$$\frac{\mathrm{d}^2 x_n}{\mathrm{d}t^2} = f\left(v_n, \Delta x_n, \Delta v_n, \mathrm{d}^2 x_{n+1}/\mathrm{d}t^2\right). \tag{3}$$

To further enhance the stability of traffic flow, Wang et al. [30] proposed a multiple speed difference model as follows:

$$\frac{\mathrm{d}^2 x_n}{\mathrm{d}t^2} = f\left(v_n, \Delta x_n, \Delta v_n, \Delta v_{n+1}, \ldots, \Delta v_{n+k}\right), \tag{4}$$

where $\Delta v_{n+i} = v_{n+i+1} - v_{n+i}$.

The above car-following models can describe some complex phenomena, but can not directly be used to study the phenomena resulted by some traffic interruption factors. In fact, each vehicle may be interrupted with some probability. Considering this, we rewrite the acceleration equation of the nth vehicle, as follows:

$$\frac{\mathrm{d}v_n(t)}{\mathrm{d}t} = \kappa\left(V\left(\Delta x_n\right) - v_n\right) + \lambda_1 p_{n+1}\left(-v_n\right) + \lambda_2\left(1 - p_{n+1}\right)\Delta v_n, \tag{5}$$

where p_{n+1} is the probability that the leading vehicle is interrupted, κ, λ_1 and λ_2 are the reactive coefficients, and $V\left(\Delta x_n(t)\right)$ is the optimal speed of the nth vehicle at time t. Once the leading vehicle is completely interrupted, its speed immediately becomes zero, *i.e.*, the speed difference between the $(n+1)$th and the nth vehicles takes $(-v_n)$. Eq. (5) states that the acceleration of the nth vehicle is determined by the speed v_n, the headway Δx_n, the relative speed Δv_n and the probability p_{n+1}.

3. The macro model

In order to study the effects that the probability of traffic interruption has on the dynamic properties of traffic flow, we should transform the micro variables in Eq. (5) into the macro ones by using the method of Ref. [22], *i.e.*,

$$\begin{aligned} &V\left(\Delta x_n(t)\right) \to v_e(\rho), \qquad v_n(t) \to v(x,t), \qquad v_{n+1}(t) \to v(x+\Delta, t), \\ &\kappa \to \frac{1}{T}, \qquad \lambda_1 \to \frac{1}{\tau_1}, \qquad \lambda_2 \to \frac{1}{\tau_2}, \qquad p_{n+1} \to p(x,t). \end{aligned} \tag{6}$$

The parameter Δ in $(x+\Delta)$ is the distance between the leading and following vehicles. The details of the inner relationship between macro and micro variables can be found in Refs. [6,9,22]. Then, Eq. (5) can be rewritten as follows:

$$\frac{\mathrm{d}v(x,t)}{\mathrm{d}t} = \frac{\partial v}{\partial t} + v\frac{\partial v}{\partial x} = \frac{v_e(\rho) - v}{T} + \frac{1}{\tau_1} p\left(-v\right) + \frac{1}{\tau_2}\left(1-p\right)\left(v\left(x+\Delta, t\right) - v\left(x,t\right)\right), \tag{7}$$

where v_e, v and ρ are respectively the equilibrium speed, the speed and the density. T, τ_1 and τ_2 are respectively the three reactive times required by drivers for adjusting their acceleration based on equilibrium speed, the speed difference $(-v)$ caused by traffic interruption and the speed difference $v\left(x+\Delta, t\right) - v\left(x,t\right)$ without traffic interruption. In general, $\kappa > \lambda_2$ and $\tau_1 < \tau_2$ hold, we then have $\tau_1 < \tau_2 < T$.

Expanding Eq. (7) by Taylor series and neglecting the nonlinear terms, we have

$$\frac{\partial v}{\partial t}+v\frac{\partial v}{\partial x}=\frac{v_e(\rho)-v}{T}+\frac{1}{\tau_1}p(-v)+\frac{\Delta}{\tau_2}(1-p)\frac{\partial v}{\partial x}. \tag{8}$$

Combining with the conservation condition of traffic flow, we obtain a new macro model with consideration of the traffic interruption probability, *i.e.*,

$$\frac{\partial U}{\partial t}+A\frac{\partial U}{\partial x}=F, \tag{9}$$

where $U=(\rho,v)^{\mathrm{T}}$, $A=\begin{pmatrix} v & \rho \\ 0 & v-c_0(1-p)\end{pmatrix}$ and $F=\left(0,\frac{v_e(\rho)-v}{T}-\frac{pv}{\tau_1}\right)^{\mathrm{T}}$. Here, $c_0=\frac{\Delta}{\tau_2}$ is the propagating speed of small perturbation. For simplicity, c_0 is assumed to be a constant in this study. Note that Eq. (9) becomes the speed gradient model proposed in Refs. [8,9] if the probability of traffic interruption is not considered.

To explore the effects that the probability of traffic interruption has on the wave properties of traffic flow, we first examine the eigenvalues of the matrix A in Eq. (9) by setting

$$\det(\lambda \mathrm{I}-\mathrm{A})=0, \tag{10}$$

where I is a 2×2 identity matrix. From Eq. (10), it follows,

$$\det\begin{pmatrix}\lambda-v & -\rho \\ 0 & \lambda-(v-c_0(1-p))\end{pmatrix}=0. \tag{11}$$

The eigenvalues are $\lambda_1=v-c_0(1-p)$ and $\lambda_2=v$ with corresponding eigenvectors $r_1=(0,1)^{\mathrm{T}}$ and $r_2=\left(1,v_e'(\rho)\right)^{\mathrm{T}}$. Eq. (9) is a strictly hyperbolic system and its characteristic speeds are not greater than the speed v, thus the anisotropy of the traffic flow can be ensured [31]. To further illustrate this, we examine the Riemann problem with the following initial values:

$$\begin{cases}\rho(x,0)=\rho_j H(x), & t=0,\\ v(x,0)=0, & t=0,\end{cases} \tag{12}$$

where $H(x)$ is a Heaviside function with $H(x)=0,\forall x<0$ and $H(x)=1,\forall x\geq 0$, and ρ_j is the jam density. Clearly, the correct solution of the system is that with these initial conditions, all vehicles remain stationary, *i.e.*, $\mathrm{d}v/\mathrm{d}t=0$. Substituting $\mathrm{d}v/\mathrm{d}t=0$ into Eq. (9), we have

$$v(x,t)=\frac{\tau_1 v_e}{\tau_1+pT}\geq 0. \tag{13}$$

Eq. (13) shows that no backward movement appears in our model.

4. Linear stability analysis

We now turn to study the effects of traffic interruption probability on the stability of traffic flow. Let (ρ^*,v^*) be the steady-state solution of Eq. (9) and $(\rho,v)=(\rho^*+\xi,v^*+\eta)$ be the perturbed solution, where $\xi(x,t)$ and $\eta(x,t)$ represent the small smooth deviations of density and speed from the steady-state solution, respectively. For simplicity, we here set the traffic interruption probability a constant. Substituting $\rho=\rho^*+\xi$ and $v=v^*+\eta$ into Eq. (9), taking the Taylor's series expansion at point (ρ^*,v^*) and neglecting the nonlinear terms, we get

$$\begin{cases}\dfrac{\partial\xi}{\partial t}+v^*\dfrac{\partial\xi}{\partial x}+\rho^*\dfrac{\partial\eta}{\partial x}=0,\\ \dfrac{\partial\eta}{\partial t}+\left(v^*-c_0(1-p)\right)\dfrac{\partial\eta}{\partial x}=\dfrac{v_e'(\rho^*)\xi-\eta}{T}-\dfrac{p(v^*+\eta)}{\tau_1}.\end{cases} \tag{14}$$

Eliminating η from Eq. (14) leads to

$$-\frac{T\tau_1}{\tau_1+Tp}[\partial_t+c_1\partial_x][\partial_t+c_2\partial_x]\xi=\xi_t+c\xi_x, \tag{15}$$

where $c_1=v^*-c_0(1-p)$ and $c_2=v^*$ are the propagation velocities of the second-order wave and $c=\frac{\tau_1(\rho^* v_e'(\rho^*)+v^*)+Tpv^*}{Tp+\tau_1}$ is the propagation speed of the first-order wave. Using the method of Jiang et al. [32], we can show that Eq. (15) is linearly stable if and only if c, c_1 and c_2 satisfies the following conditions

$$c_1\leq c\leq c_2. \tag{16}$$

If Eq. (16) is not satisfied, unstable stop and go traffic may appear. The following theorem gives the condition for improving traffic flow stability when considering the traffic interruption probability.

Theorem 1. *The consideration of traffic interruption probability can improve the stability of traffic flow if and only if the parameters satisfy* $\tau_1 \le T(1-p)$.

Proof. It has been known that the condition for traffic flow stability is $\rho_0 v_e'(\rho_0) \ge -c_0$ when the traffic interruption probability is not considered. In addition, Eq. (16) can be rewritten as $\rho_0 v_e'(\rho_0) \ge -c_0(1-p) - \frac{Tpc_0(1-p)}{\tau_1}$. It is clear that $-c_0 \ge -c_0(1-p) - \frac{Tpc_0(1-p)}{\tau_1}$ is equivalent to $\tau_1 \le T(1-p)$. Thus, $\rho_0 v_e'(\rho_0) \ge -c_0 \ge -c_0(1-p) - \frac{Tpc_0(1-p)}{\tau_1}$ is equivalent to $\tau_1 \le T(1-p)$. This shows that the new model with consideration of traffic interruption probability can improve the traffic flow stability if and only if $\tau_1 \le T(1-p)$. □

In order to further explain Theorem 1, we divide the reactive time T in Eq. (7) into such two parts as Tp and $T(1-p)$. Tp and $T(1-p)$ are respectively the reactive times required by drivers for adjusting their acceleration based on the speed difference $v_e - v$ caused by traffic interruption probability p and non-interruption probability $1-p$. Theorem 1 shows that our model can improve the stability of traffic flow if and only if the reactive time τ_1 is not larger than the reactive time $T(1-p)$. If the probability of traffic interruption $p = 1$ (*i.e.*, traffic is interrupted everywhere), Theorem 1 states that τ_1 will be equal to zero in order to improve the stability of traffic flow. The acceleration will immediately become infinite and the speeds of all vehicles will immediately be zero. If there is no traffic interruption everywhere (*i.e.*, $p = 0$), our model is just the speed gradient model [8,9]. Note that the fact $T(1-p)$ decreases with the increase of traffic interruption probability p, doesn't mean the stable region is reduced. The condition $\tau_1 \le T(1-p)$ ensures that, when the traffic interruption probability p is increased, τ_1 must drop. This implies that the effects of the term $\frac{1}{\tau_1} p(-v)$ on car-following behavior are enhanced with the increase of traffic interruption probability p.

5. Simulation results

Zhang et al. [33–35] pointed out that the conservative scheme is a good choice for carrying out numerical tests if using dynamics model to describe traffic flow. Hence, we rewrite Eq. (9) as follows:

$$\frac{\partial u}{\partial t} + \frac{\partial f(u)}{\partial x} = s(u), \tag{17}$$

where $u = (\rho, v)^{\mathrm{T}}, f(u) = \left(\rho v, 0.5v^2 - c_0(1-p)v\right)^{\mathrm{T}}, s(u) = \left(0, \frac{v_e - v}{T} - \frac{pv}{\tau_1}\right)^{\mathrm{T}}$. We adopt the following conservative scheme to discretize Eq. (17)

$$u_i^{n+1} = u_i^n - \frac{\Delta t}{\Delta x}(\hat{f}_{i+1/2}^n - \hat{f}_{i-1/2}^n) + s(u_i^n)\Delta t, \tag{18}$$

where $\hat{f}_{i+1/2}^n = \hat{f}(u_i^n, u_{i+1}^n)$ is the local Lax-Friedrichs flow, *i.e.*,

$$\hat{f}(u_i^n, u_{i+1}^n) = \frac{1}{2}\left(f(u_i^n) + f(u_{i+1}^n) - \alpha(u_{i+1}^n - u_i^n)\right), \tag{19}$$

where α is the maximum characteristic speed of Eq. (9). For simplicity, we set $\alpha = v_f$. In addition, i and n are the space and time indexes, respectively; Δx and Δt are the spatial and time steps, respectively.

5.1. Shock waves and rarefaction waves

We now investigate the effects that the traffic interruption probability and one traffic interruption (*e.g.*, accident) have on the formation and propagation of a shock wave and a rarefaction wave. The initial conditions are as follows:

$$\begin{cases} \rho_{\mathrm{up}}^1 = 0.04 \text{ veh/m}, & \rho_{\mathrm{down}}^1 = 0.18 \text{ veh/m}, \\ \rho_{\mathrm{up}}^2 = 0.18 \text{ veh/m}, & \rho_{\mathrm{down}}^2 = 0.04 \text{ veh/m}, \end{cases} \tag{20}$$

where ρ_{up}^1 and ρ_{down}^1 are respectively the upstream and downstream densities in the case of shock wave; ρ_{up}^2 and ρ_{down}^2 are respectively the upstream and downstream densities in the case of rarefaction wave. The initial speeds are set below:

$$v_{\mathrm{up}}^i = v_e\left(\rho_{\mathrm{up}}^i\right), \qquad v_{\mathrm{down}}^i = v_e\left(\rho_{\mathrm{down}}^i\right), \quad i = 1, 2. \tag{21}$$

Free boundary condition, *i.e.*, $\partial\rho/\partial x = \partial u/\partial x = 0$, are employed. The equilibrium speed function is [36]:

$$v_e(\rho) = v_f\left[1 - \exp\left(1 - \exp\left(\frac{c_m}{v_f}\left(\frac{\rho_j}{\rho} - 1\right)\right)\right)\right], \tag{22}$$

where v_f is the free flow speed, c_m is the speed of the kinematic wave under the jam density, and ρ_j is the jam density. In this section, the road length used for simulation is 20 km and the discontinuous point (*i.e.*, the location demarcating upstream

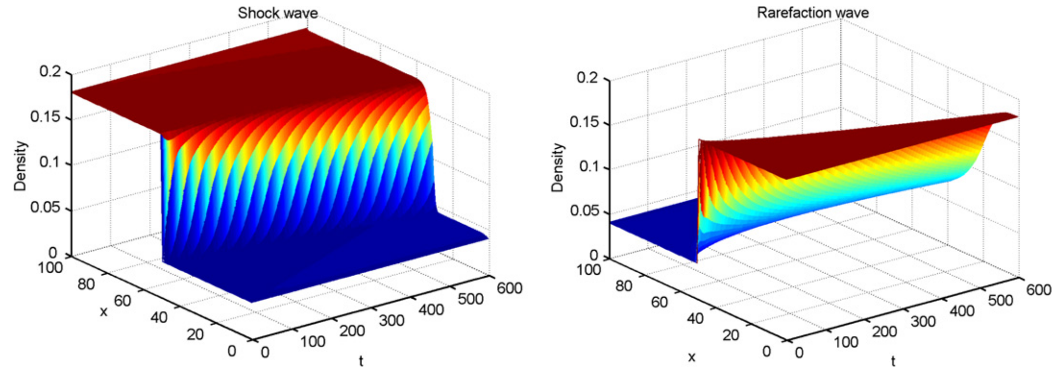

Fig. 1. Evolution of shock wave and rarefaction wave with consideration of the traffic interruption probability.

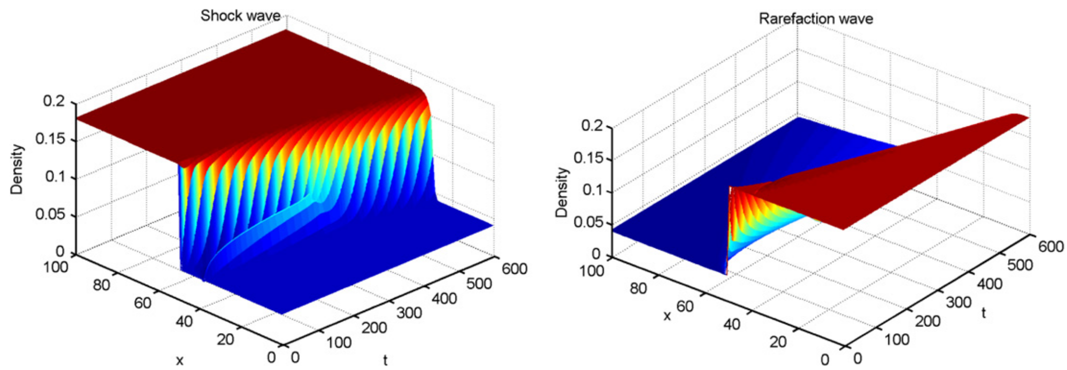

Fig. 2. Evolution of shock wave and rarefaction wave when accident occurs at the upstream of the discontinuous point.

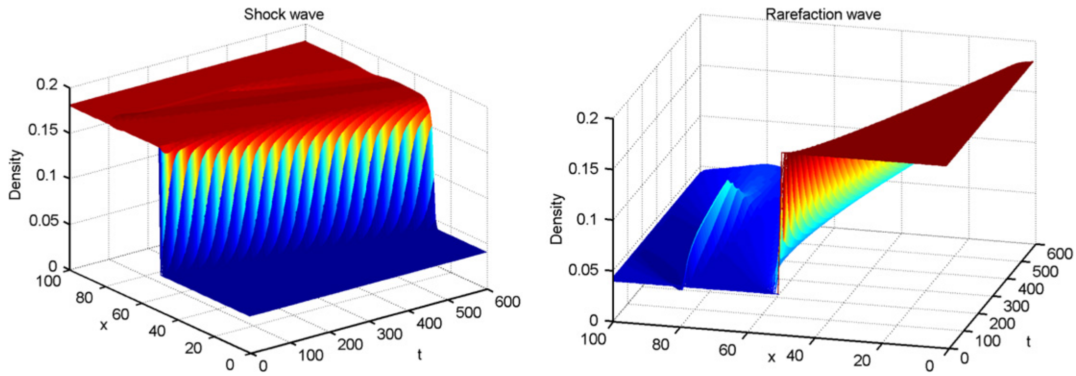

Fig. 3. Evolution of shock wave and rarefaction wave when accident occurs at the downstream of the discontinuous point.

and downstream densities in Eq. (20)) is at the middle of the road. The values of these parameters are: $c_0 = c_m = 11$ m/s, $T = 10$ s, $v_f = 30$ m/s, $\rho_j = 0.2$ veh/m, $\tau_1 = 8$ s, $p = 0.2$, $\Delta x = 200$ m and $\Delta t = 1$ s.

Fig. 1 depicts the density evolution in these two cases. The following observations can be made from this figure:

(i) The results are similar to that reported in Refs. [6–8], so the new model can reasonably describe the formation and propagation of a shock wave and a rarefaction wave.

(ii) The consideration of traffic interruption probability can smooth the front of the shock wave and slow down its propagating speed, but has little effect on the rarefaction wave.

We then explore the effects that one traffic interruption (*e.g.*, accident) has on the two traffic waves in two situations: (a) the accident appears at $x = 4$ km (the upstream of the discontinuous point) and lasts for as long as 5 min; (b) the accident occurs at $x = 16$ km (the downstream of the discontinuous point) and lasts for as long as 5 min.

Figs. 2 and 3 show the density evolution in these two situations. We can find the following points from these two figures:

(i) When an accident appears at the upstream of the discontinuous point, the rarefaction wave is influenced little since the clustering vehicles can be quickly dissipated. The accident can slow down the propagating speed of shock wave and make the wavefront smoother than that without the accident. The backward propagating cluster appears at the upstream of the accident. There is an intention to generate new traffic waves when the duration of the accident is further increased (see Fig. 2).

(ii) When an accident appears at the downstream of the discontinuous point, both the shock and rarefaction waves are affected a little, but the backward propagating cluster occurs at the upstream of the accident. The cluster becomes obvious and new traffic waves emerge when the duration of the accident is further increased (see Fig. 3).

(iii) The above results are accordant with real traffic, so the new model can be used to describe traffic with an accident.

5.2. Small disturbance analyses

It has been well known that a small disturbance may generate stop-and-go traffic under some conditions. We now investigate the time-space evolution of the flow density when the probability of traffic interruption is taken into account in our model. We adopt the following initial condition [37]:

$$\rho(x,0)=\rho_0+\Delta\rho\left\{\cosh^{-2}\left(\frac{160}{L}\left(x-\frac{5L}{16}\right)\right)-\frac{1}{4}\cosh^{-2}\left(\frac{40}{L}\left(x-\frac{11L}{32}\right)\right)\right\}, \tag{23}$$

where the first term is the initial density, the second term is the disturbance, and L is the length of the road section. In the following simulation, let $L = 32.2$ km and use the periodic boundary conditions, *i.e.*,

$$\rho(0,t)=\rho(L,t),\qquad v(0,t)=v(L,t). \tag{24}$$

We adopt the following equilibrium speed function [38]:

$$v_e=v_e(\rho)=v_f\left(1\Big/\left(1+\exp\left(\frac{\rho/\rho_j-0.25}{0.06}\right)\right)-3.72\times 10^{-6}\right). \tag{25}$$

In addition, set the initial speed $v(x,0)=v_e(\rho(x,0))$, $\Delta\rho=0.01$, the space step $\Delta x=100$ m, and the time step $\Delta t=1$ s. Other parameters are identical to those used in Section 5.1.

Theorem 1 shows that the consideration of traffic interruption probability can improve the stability of traffic flow if and only $\tau_1\le T(1-p)$. The unstable region of traffic flow can be analytically obtained by substituting the parameters into Eq. (16). This region is the same as that given in Ref. [9]. Numerical results show that the unstable region given by our model is $0.042<\rho_0<0.075$. In comparison with $0.031<\rho_0<0.084$ which is the region without considering the traffic interruption probability, our model reduces the unstable region.

The evolution of small perturbation is shown in Fig. 4. We have the following findings from this figure:

(i) When traffic is light or heavy, *i.e.*, the initial density is less than the lower critical density 0.042 or greater than the upper critical density 0.075, the small perturbation is dissipated without any amplification (see Fig. 4(a) and (e)). When the initial density is in the unstable region, the small perturbation is amplified and eventually leads to traffic instability (see Fig. 4(b)–(d)). These findings were also reported by Jiang et al. [9].

(ii) For $0.031<\rho_0<0.042$ and $0.075<\rho_0<0.084$, stop-and-go traffic doesn't occur because the probability of traffic interruption is considered (see Fig. 4(b) and (e)). Thus, our model can improve the stability of the traffic flow.

(iii) When the initial density is in the stable region, the consideration of traffic interruption probability can speed up the propagation of the second-order and the first-order waves but stop-and-go traffic never appears (see Fig. 4(a), (b) and (e)) since there are no conflicts between the propagating processes of the first-order and the second-order waves [32]. When the initial density is in the unstable region, the stop-and-go traffic occurs (see Fig. 4(c) and (d)) since there exist some conflicts between the propagating processes of the first-order and the second-order waves. However, the consideration of traffic interruption probability can relieve the conflicts, so the stop-and-go traffic is not as obvious as that in Ref. [9].

Next, we turn to study the effects that one traffic interruption (*e.g.*, accident) has on uniform flow. For simplicity, we assume that only one accident occurs at $x=10$ km and lasts for as long as 300 s. Other parameters and conditions are the same as those in Fig. 4. The evolution of uniform flow is shown in Fig. 5. The following observations can be made:

(i) When the initial density is low ($0\le\rho_0<0.03$), the accident has little effect on uniform flow and a slight cluster appears only at the accident position and can be dissipated quickly (see Fig. 5(a)).

(ii) For $0.03\le\rho_0<0.042$, a cluster appears. The cluster becomes more serious and its propagating speed increases with the accident tracking time (see Fig. 5(b)).

(iii) For $0.042\le\rho_0<0.08$, stop-and-go traffic appears. This verifies that an accident can wreck uniform flow and produce stop-and-go traffic when the initial density is in the unstable region (see Fig. 5(c)–(e)).

(iv) When $\rho_0\ge 0.08$, traffic becomes uniform flow again. This means that the accident has little effect on uniform flow because the speed is so small that accident cannot produce a cluster (see Fig. 5(f)).

Note that the stop-and-go in Figs. 4 and 5 is not as serious as that in Ref. [9], thus our model is able to improve the stability of the traffic flow.

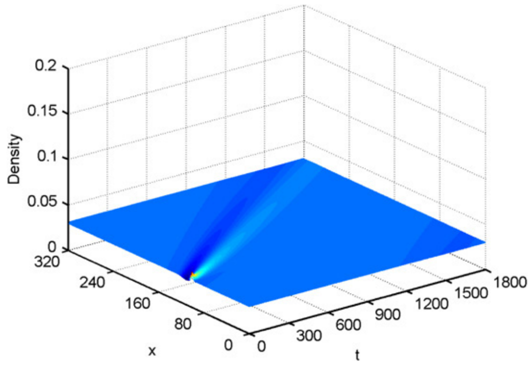

(a) $\rho_0 = 0.03$.

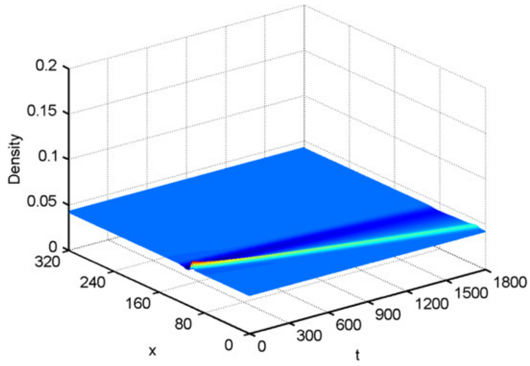

(b) $\rho_0 = 0.042$.

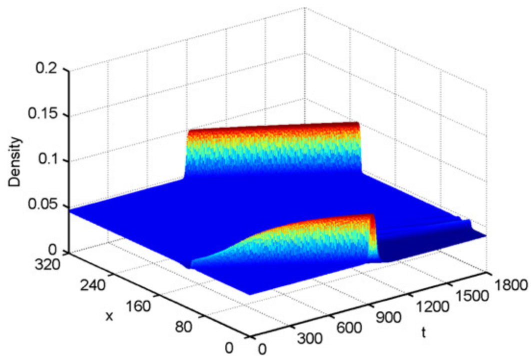

(c) $\rho_0 = 0.046$.

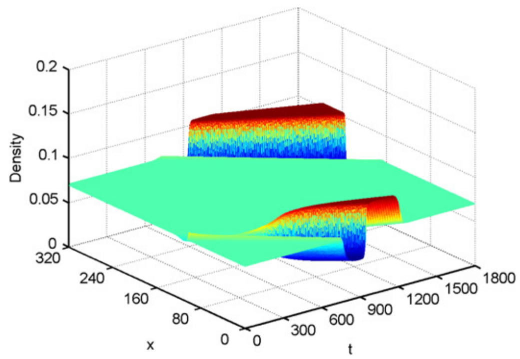

(d) $\rho_0 = 0.07$.

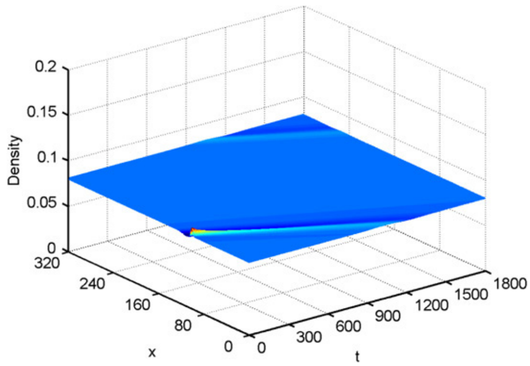

(e) $\rho_0 = 0.08$.

Fig. 4. Evolution of small perturbation with consideration of the accidental probability.

6. Other cases

Simulation results presented in Section 5 show that the probability of traffic interruption and one traffic interruption (*e.g.*, accident) have of effecting traffic flow, and our model can describe various complex traffic phenomena associated with an accident. In this section, we apply the new model to further reproduce some complex traffic phenomena resulted by other traffic interruptions, such as signal lights, tolling stations and pedestrians.

Case I: Suppose a traffic system with one signal light. Traffic is interrupted by a red signal and the length of red signal is the last time of the traffic interruption. Then, our model can directly be used to study the effect of a signal light on traffic as long as the probability of traffic interruption is formulated as follows:

$$p(x,t) = \begin{cases} 1, & \text{if } x \text{ is the signal position and } 0.5(n-1)C < t \le 0.5nC, \\ 0, & \text{else}, \end{cases} \tag{26}$$

where $C = 60$ s is the cycle time with red-to-green ratio (1:1), n is the number of times that vehicles meet with red signal. Numerical results are shown in Figs. 6 and 7, corresponding to a ring road and an open road respectively. From Fig. 6, we

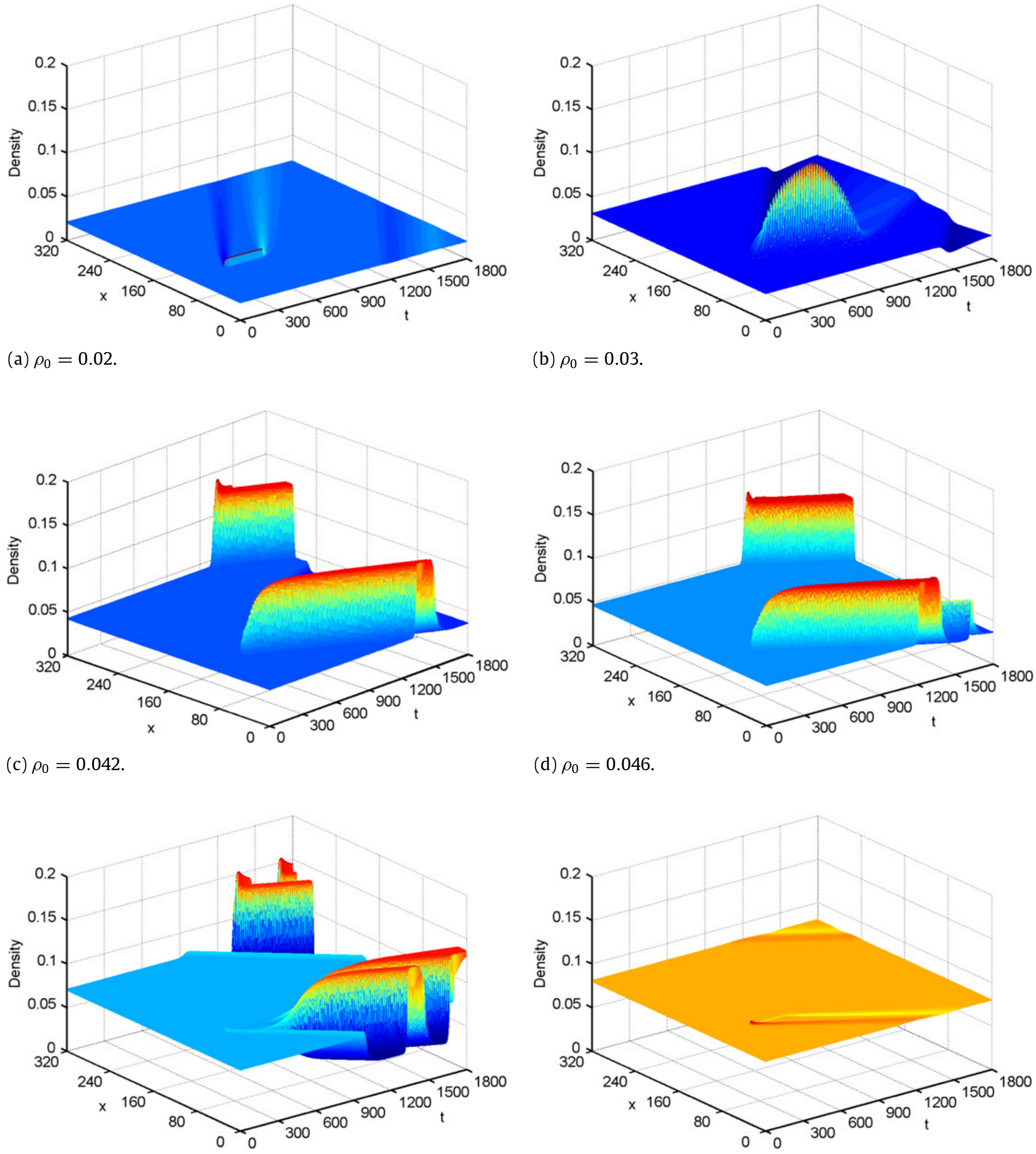

(a) $\rho_0 = 0.02$.

(b) $\rho_0 = 0.03$.

(c) $\rho_0 = 0.042$.

(d) $\rho_0 = 0.046$.

(e) $\rho_0 = 0.07$.

(f) $\rho_0 = 0.08$.

Fig. 5. Evolution of uniform flow when one traffic interruption (*e.g.*, accident) occurs.

get the following findings:

(i) For $0 \le \rho_0 \le 0.025$, the signal light has little effect on traffic flow. The traffic flow is stable and slight cluster appears only at the signal light (see Fig. 6(a)).

(ii) For $0.025 \le \rho_0 \le 0.08$, the signal light can wreck the stability of traffic flow. A local cluster propagating backward appears when $0.025 \le \rho_0 \le 0.042$ (see Fig. 6(b)) and serious stop-and-go occurs when $0.042 \le \rho_0 \le 0.08$ (see Fig. 6(c)–(e)). The cluster and the stop-and-go caused by the signal light will become more serious with the increasing duration of the red signal.

(iii) For $0.08 \le \rho_0 \le 0.2$, the signal light has little effect on traffic flow and generates a slight cluster propagating backward (see Fig. 6(f)).

From Fig. 7, we have the following observations:

(i) For $0 \le \rho < 0.04$, the signal light only produces some slightly oscillating waves propagating backward and the downstream density slightly drops during the red time period (see Fig. 7(a)). The oscillating waves will become more serious with the increasing duration of the red signal.

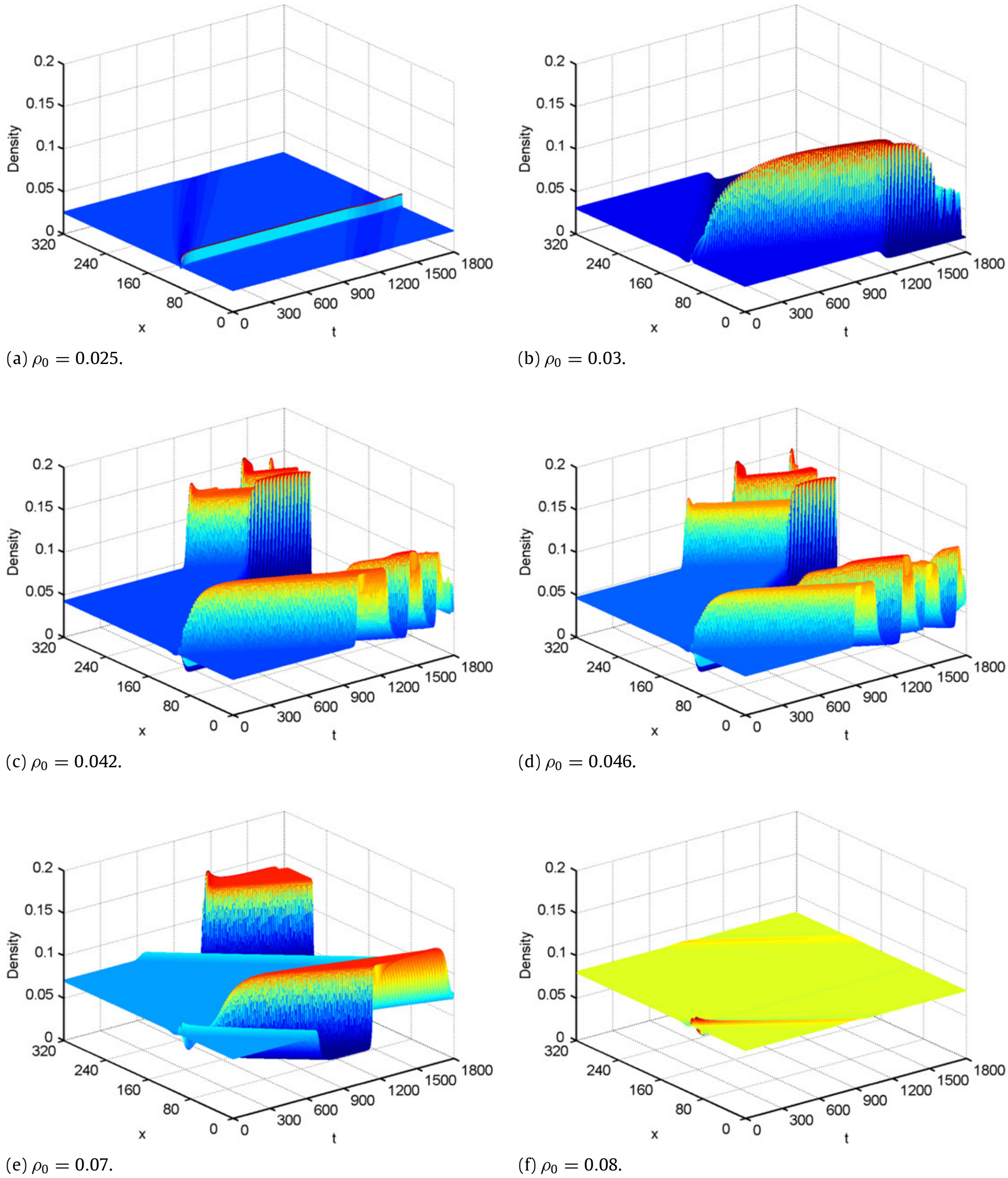

(a) $\rho_0 = 0.025$.

(b) $\rho_0 = 0.03$.

(c) $\rho_0 = 0.042$.

(d) $\rho_0 = 0.046$.

(e) $\rho_0 = 0.07$.

(f) $\rho_0 = 0.08$.

Fig. 6. Density evolution on a ring road with a signal light located at $x = 10$ km.

(ii) For $0.04 \le \rho < 0.2$, the signal light produces a serious cluster propagating backward (see Fig. 7(b)) and the cluster will become more serious with the increasing duration of the red signal.

Case II: A driver has to immediately brake when there are pedestrians crossing the road in front. The crossing action can be regarded as a traffic interruption and the last time of the traffic interruption is the time required for crossing the road. We can then apply our model to analyze the effects that the crossing action has on traffic flow. The probability of a traffic interruption can be defined below:

$$p(x, t) = \begin{cases} 1, & \text{if } x \text{ is the crossing position and } (n-1)r < t \le (n-1)r + t_{\text{cross}}, \\ 0, & \text{else}, \end{cases} \tag{27}$$

where $1/r$ ($r = 60$ s) is the arrival rate of pedestrians, $t_{\text{cross}} = 10$ s is the time required for crossing the road and n is the number of times that pedestrians cross the road. Simulation results are shown in Fig. 8. It can be seen that both oscillating waves and a cluster appear due to the pedestrians' crossing action. They will become more serious with the increasing arrival

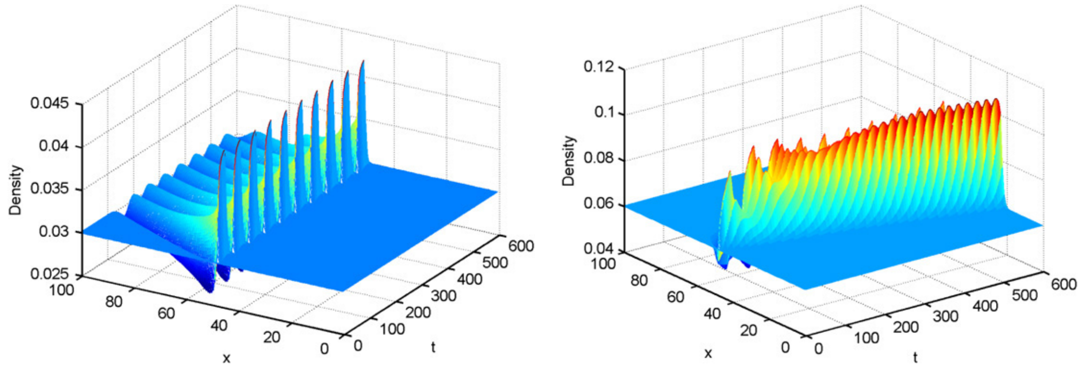

(a) $\rho_0 = 0.03$. (b) $\rho_0 = 0.06$.

Fig. 7. Density evolution on an open road with a signal light located at $x = 5$ km.

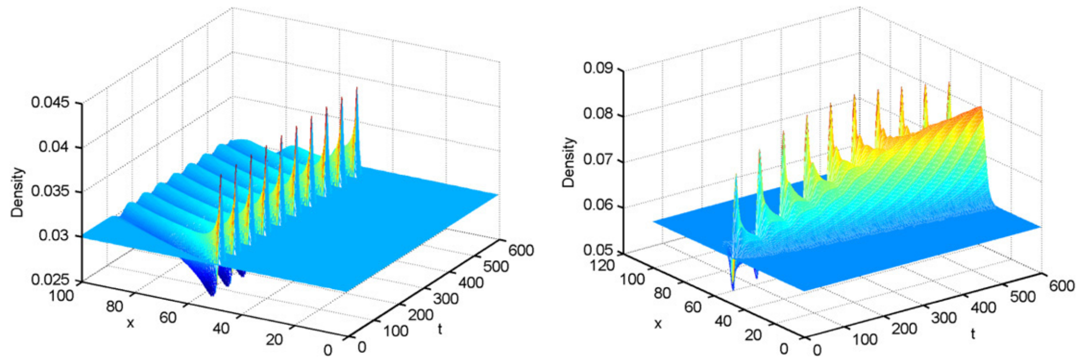

(a) $\rho_0 = 0.03$. (b) $\rho_0 = 0.06$.

Fig. 8. Density evolution on an open road with a zebra crossing located at $x = 5$ km.

rate of pedestrians. Clearly, a flyover should be constructed for reducing the effects of crossing pedestrians on traffic flow when the arrival rate is relatively high.

Case III: Consider a tolling station where drivers stop and pay to go through. It should be noted that the time for paying and the frequency of tolling are related to the traffic density. For simplicity, we define their relationships as follows:

$$\begin{cases} t_{\text{tolling}} = 5\ \text{s} \quad \text{and} \quad t_{\text{period}} = 100\ \text{s}, & \text{if } \rho\left(x_0, t\right) \le 0.02, \\ t_{\text{tolling}} = 10\ \text{s} \quad \text{and} \quad t_{\text{period}} = 50\ \text{s}, & \text{if } 0.02 < \rho\left(x_0, t\right) \le 0.04, \\ t_{\text{tolling}} = 15\ \text{s} \quad \text{and} \quad t_{\text{period}} = 25\ \text{s}, & \text{if } \rho\left(x_0, t\right) > 0.02, \end{cases} \tag{28}$$

where $x_0 = 5$ km is the position of the tolling station, t_{tolling} is the tolling time and $1/t_{\text{period}}$ is the frequency of tolling. The accurate relationships among t_{tolling}, $1/t_{\text{period}}$ and ρ have to be calibrated using the survey data although Eq. (28) reflects a basic fact. Then, the probability of traffic interruption on a road with one tolling station can be defined as follows:

$$p\left(x_0, t\right) = \begin{cases} 1, & \text{if } t_0 + (n-1)\, t_{\text{period}} \le t < t_0 + (n-1)\, t_{\text{period}} + t_{\text{tolling}}, \\ 0, & \text{else}, \end{cases}, \tag{29}$$

where n is the number of times for tolling. Simulation results are shown in Fig. 9. It can be seen that the density evolution in this case is similar to that observed on an open road in Case I (see Fig. 7). The following findings are obtained through comparing Figs. 7 and 9:

(i) When the initial density is relatively low, the frequency of oscillating waves is less than that in Fig. 7. This is because both the frequency of tolling and the length of tolling time are respectively less than the frequency of red signals and the duration of the red signals (see Fig. 7(a) and Fig. 9(a)).

(ii) When initial density is relatively high, the density at the downstream of the tolling station goes down greatly and the propagating speed of the cluster caused by tolling increases significantly (see Fig. 9(b)).

7. Conclusions

There are few traffic flow models to study the effects that the probability of traffic interruption and various traffic interruptions (*e.g.*, accident, signal light, pedestrian and tolling station) have on traffic flow. In this paper, we presented

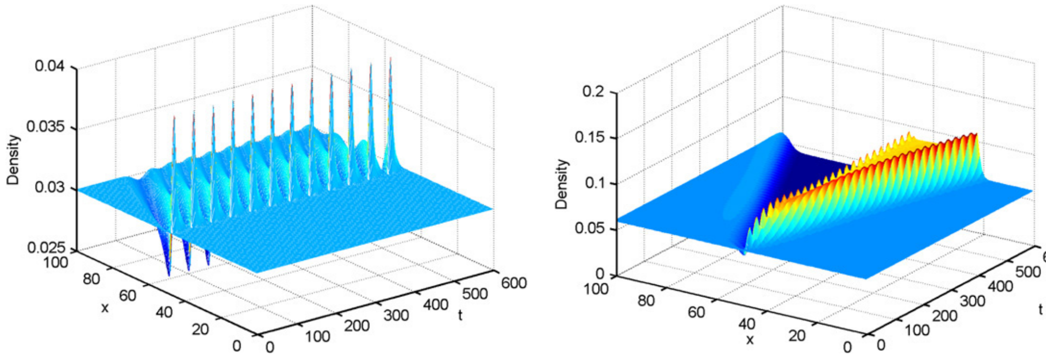

(a) $\rho_0 = 0.03$.

(b) $\rho_0 = 0.06$.

Fig. 9. Density evolution on an open road with one tolling station located at $x = 5$ km.

a new macro model which involves the effects of traffic interruption probability on car-following behavior through formulating the inner relationship between the micro and the macro variables. Linear stability analysis of the model was conducted and it was proven that consideration of the traffic interruption probability can improve the stability of traffic flow if and only if the drivers' reactive time required for adjusting their acceleration based on the traffic interruption probability p is not greater than that one based on the non-interruption probability $1 - p$. Simulation results further verified that the new model can reasonably describe various complex traffic phenomena caused by various traffic interruptions. Regarding each traffic interruption, we have identified the main factors contributing to the effects. These factors include: the probability function of traffic interruption, the position and the last time of traffic interruption, the cycle and the split of signal light, the pedestrians' arrival rate and the time for crossing road, the tolling time and the tolling frequency, as well as the traffic density.

The results reported in this paper rely on the assumed values of all parameters. It is of interest to calibrate these parameters by survey data in order to optimize the performance of the model. In addition, the current work is limited in one-road system, extending it to a road network would be both valuable and challenging.

Acknowledgments

The work described in this paper is jointly supported by the National Natural Science Foundation of China (70701002, 70521001) and the National Basic Research Program of China (2006CB705503). The authors would like to thank anonymous referees for their helpful comments and valuable suggestions which improved the content and composition substantially.

References

[1] D. Chowdhury, L. Santen, A. Schreckenberg, Phys. Rep. 319 (2000) 199.
[2] M.J. Lighthill, G.B. Whitham, Proc. R. Soc. 229 (1955) 281.
[3] P.I. Richards, Oper. Res. 4 (1956) 42.
[4] D.F. Daganzo, Transp. Res. B 31 (1997) 83.
[5] G.C.K. Wong, S.C. Wong, Transp. Res. A 36 (2002) 827.
[6] H.M. Zhang, Transp. Res. B 32 (1998) 485.
[7] A. Aw, M. Rascle, SIAM J. Appl. Math. 60 (2000) 916.
[8] R. Jiang, Q.S. Wu, Z.J. Zhu, Chinese Sci. Bull. 46 (2001) 345.
[9] R. Jiang, Q.S. Wu, Z.J. Zhu, Transp. Res. B 36 (2002) 405.
[10] C.F. Tang, R. Jiang, Q.S. Wu, Chin. Phys. 16 (2007) 1570.
[11] Y. Xue, S.Q. Dai, Phys. Rev. E 68 (2003) 066123.
[12] A.K. Gupta, V.K. Katiyar, Transportmetrica 3 (2007) 73.
[13] T.Q. Tang, H.J. Huang, Chinese Sci. Bull. 49 (2004) 2097.
[14] H.J. Huang, T.Q. Tang, Z.Y. Gao, Acta Mech. Sin. 22 (2006) 132.
[15] T.Q. Tang, H.J. Huang, S.C. Wong, X.Y. Xu, Physica A 376 (2007) 649.
[16] T.Q. Tang, H.J. Huang, Y. Xue, Acta Phys. Sinica 55 (2006) 4026 (in Chinese).
[17] S.C. Wong, B.S.Y. Leung, B.P.Y. Loo, W.T. Hung, H.K. Lo, Accident Anal. Prev. 36 (2004) 281.
[18] S.C. Wong, N.N. Sze, Y.C. Li, Accident Anal. Prev. 39 (2007) 1107.
[19] N.N. Sze, S.C. Wong, Accident Anal. Prev. 39 (2007) 1267.
[20] L. Telesca, M. Lovallo, Physica A 387 (2008) 3299.
[21] M. Baykal-Gürsoy, W. Xiao, K. Ozbay, European J. Oper. Res. (in press).
[22] G.Q. Liu, A.S. Lyrintiz, P.G. Michalopoulos, Transp. Res. Rec. 1644 (1998) 37.
[23] T. Nagatani, Phys Rev. E 60 (1999) 6395.
[24] H. Lenz, C.K. Wagner, R. Sollacher, Eur. Phys. J. B 7 (1999) 331.
[25] K. Hasebe, A. Nakayama, Y. Sugiyama, Phys. Rev. E 68 (2003) 026102.
[26] K. Hasebe, A. Nakayama, Y. Sugiyama, Phys. Rev. E 69 (2004) 017103.
[27] H.X. Ge, S.Q. Dai, L.Y. Dong, Y. Xue, Phys. Rev. E 70 (2004) 066134.
[28] X.M. Zhao, Z.Y. Gao, Eur. Phys. J. B 47 (2005) 145.
[29] R. Jiang, Q.S. Wu, Z.J. Zhu, Phys. Rev. E 64 (2001) 017101.

[30] T. Wang, Z.Y. Gao, X.M. Zhao, Acta Phys. Sinica 55 (2006) 634 (in Chinese).
[31] C.F. Daganzo, Transp. Res. B 29 (1995) 277.
[32] R. Jiang, Q.S. Wu, Z.J. Zhu, Appl. Math. Mech. 23 (2002) 409.
[33] P. Zhang, R.X. Liu, S.C. Wong, Phys. Rev. E 71 (2005) 056704.
[34] P. Zhang, S.C. Wong, Phys. Rev. E 74 (2006) 026109.
[35] P. Zhang, S.C. Wong, S.Q. Dai, Chin. Phys. Lett. 23 (2006) 516.
[36] Del J.M. Castillo, F.G. Benitez, Transp. Res. B 29 (1995) 373.
[37] M. Herrmann, B.S. Kerner, Physica A 255 (1998) 163.
[38] B.S. Kerner, P. Konhäuser, Phys. Rev. E 48 (1993) R2335.